

AMES-HET-97-06  
May 1997

## $b\bar{b}$ Production on the $Z$ Resonance and Implications for LEP2

A. Datta<sup>a</sup>, K. Whisnant<sup>a</sup>, Bing-Lin Young<sup>a</sup>, and X. Zhang<sup>b</sup>

<sup>a</sup>*Department of Physics and Astronomy, Iowa State University, Ames, IA 50011, USA*

<sup>b</sup>*Institute of High Energy Physics, Beijing 100039, P.R. China*

### Abstract

In terms of an effective lagrangian, we examine the effect of new physics associated with third-generation fermions on  $b\bar{b}$  production at the  $Z$  resonance and study its implications for LEP2. We obtain the constraints on such operators with derivative couplings at LEP1 and the SLC, and determine the prospects for detecting their presence at LEP2. We find that despite the small observed deviations from the standard model on the  $Z$  resonance, much larger deviations from standard model predictions are possible at LEP2, and the corresponding couplings can be determined rather precisely.

## I. INTRODUCTION

Although the Standard Model (SM) has been tremendously successful in describing the physics of the electroweak interactions [1], it is quite possible that it is only an effective theory which at higher energies will break down as the deeper structure of the underlying physics emerges. There are reasons to believe that the deviation from the standard model might first appear in the interactions involving the third-generation fermions [2]. The large value of the top quark mass [3], on the order of the Fermi scale, means that the top quark couples significantly to the electroweak symmetry-breaking sector. Considerations of “triviality” [4] and “naturalness” [5] suggest that the scalar sector of the full theory may be more complicated than the one in the standard model. If so, the Higgs sector of the SM may be described by an effective theory which will most likely induce new physics interactions for the third-generation fermions. In fact, there are subtle deviations from standard model predictions for measurements involving the  $b$ -quark on the  $Z$  resonance [6], which, if they persist, could be an indication of new physics beyond the standard model.

In this paper we examine the new physics effects on  $b\bar{b}$  production at the  $Z$  resonance and its implications for LEP2 in terms of an effective lagrangian. Specifically, we focus on a class of CP-conserving dimension-six operators which can contribute to  $e^+e^- \rightarrow b\bar{b}$ , and which involve a derivative coupling. Such operators in principle can be detected at LEP1 and the SLC, and their influence will increase at higher energies. We determine the limits on the operators which contribute to  $e^+e^- \rightarrow b\bar{b}$  from the precision data at LEP1 and the SLC, and from partial-wave unitarity considerations. We find that the data slightly favors nonzero values of the anomalous couplings. Then we determine the range of possible measurements at LEP2 allowed by these constraints, and show how one might determine which operators are present if deviations from SM predictions are observed at LEP2.

There are two kinds of effective lagrangians used in the literature to describe the new physics of the top quark. In the so-called linear realization, an explicit Higgs doublet of the SM is included and electroweak symmetry breakdown is assumed to be induced by the Higgs

potential as in the SM. In this effective lagrangian, the leading terms are given by the SM and the corrections which come from the underlying theory beyond the SM are described by higher dimension operators. So the SM will be recovered in the limit  $\Lambda \rightarrow \infty$  and the mass of the Higgs boson is constrained by the "vacuum stability" [7] and "triviality" [8] arguments. In the second common approach, the effective lagrangian with a non-linearly realization of the SM symmetry, one constructs non-linear fields from the fermions, such as the top quark, and the would-be goldstone bosons which give masses to the W and Z bosons. Without an explicit Higgs doublet in the model, electroweak symmetry breakdown in the nonlinear realization is generally assumed, but no specific mechanism needs to be given. In this effective lagrangian the leading terms are again the SM, and the corrections, which come from the underlying theory responsible for the symmetry breaking and mass generation, are described by higher dimension operators and also by dimension-4 operators, which is *different* from the linear realization of the effective lagrangian. A Higgs field, as a singlet scalar, can be easily added to the lagrangian, but its couplings to the matter fields will not be constrained by the mass of the latter.

In this paper we take an effective lagrangian with a linear realization of the SM symmetry. In Refs. [9] and [10], the higher dimension operators which involve fermions of the third generation, gauge bosons, and Higgs bosons and which conserve CP are given. Here we will restrict the list of the higher dimension operators to those which lead to changes in  $e^+e^- \rightarrow b\bar{b}$  (since these are accessible on the Z resonance) and involve a derivative coupling. These operators are

$$\Delta\mathcal{L} = \frac{1}{\Lambda^2} [ c_{1L}g_2\bar{\Psi}_L\gamma_\mu\tau_a\Psi_L(D_\nu W^{\mu\nu})^a + c_{3L}g_1\bar{\Psi}_L\gamma_\mu\Psi_LD_\nu B^{\mu\nu} + \tilde{c}_{3R}g_1\bar{b}_R\gamma_\mu b_R D_\nu B^{\mu\nu} \\ + (c_{bW}g_2\bar{\Psi}_L\sigma^{\mu\nu}\tau_a\Phi b_R W_{\mu\nu}^a + c_{bB}g_1\bar{\Psi}_L\sigma^{\mu\nu}\Phi b_R B_{\mu\nu} + c_{Db}\bar{\Psi}_L D_\mu b_R D^\mu\Phi + H.c.) ]. \quad (1)$$

where  $\Psi_L = (t, b)_L$  and  $c_{1L}, c_{3L}$ , etc., are free parameters determining the strength of the corresponding operators in the effective lagrangian. The contributions of these operators will be enhanced relative to the standard model in processes with higher CM energy than LEP1 and the SLC, such as at LEP2.

This paper is organized as follows. In Sec. II we will examine the current constraints on these operators from LEP1 and the SLC, and in Sec. III we will find the limits on these operators from partial wave unitarity. In Sec. IV we will determine their possible effects at LEP2. A brief discussion is given in Sec. V. Finally, details for obtaining the bounds from partial wave unitarity are presented in the Appendix.

## II. CONSTRAINTS ON THE $Z$ RESONANCE

The effective Lagrangian for  $e^+e^- \rightarrow b\bar{b}$  which arises from the Standard Model plus the anomalous interactions listed above can be written

$$\begin{aligned} \mathcal{L}^{eff} = & \bar{e}_L \gamma_\mu e_L \bar{b} \left[ G_{LL} \gamma^\mu \Gamma_L + G_{LR} \gamma^\mu \Gamma_R + G_{LS} \frac{p_1^\mu - p_2^\mu}{\sqrt{s}} - i G_{LT} \sigma^{\mu\nu} \frac{p_1^\nu + p_2^\nu}{\sqrt{s}} \right] b \\ & + \bar{e}_R \gamma_\mu e_R \bar{b} \left[ G_{RL} \gamma^\mu \Gamma_L + G_{RR} \gamma^\mu \Gamma_R + G_{RS} \frac{p_1^\mu - p_2^\mu}{\sqrt{s}} - i G_{RT} \sigma^{\mu\nu} \frac{p_1^\nu + p_2^\nu}{\sqrt{s}} \right] b, \end{aligned} \quad (2)$$

where (for convenience, a momentum instead of a partial derivative in the effective lagrangian is used)  $p_1$  and  $p_2$  refer to the momenta of the final state  $b$  and  $\bar{b}$  quarks, respectively. We note that although the terms involving  $\bar{b}(p_1^\mu - p_2^\mu)b$  can be transformed into a linear combination of the other terms in  $\mathcal{L}^{eff}$  using the Gordon decomposition, we keep them here since they arise from independent anomalous operators with different top quark couplings. Also, terms involving  $\bar{b}(p_1^\mu + p_2^\mu)b$  and  $\bar{b}(-i\sigma^{\mu\nu})(p_1^\nu - p_2^\nu)b$  (which are equal to each other by the Gordon decomposition) are not included since their contributions to the matrix element are proportional to the electron mass and therefore negligible.

In terms of the couplings defined above

$$G_{LL} = \frac{e^2}{s} \left[ \frac{1}{3} + \frac{s}{\Lambda^2} (-c_{1L} + c_{3L}) \right] + \frac{g_Z^2 (-\frac{1}{2} + s_W^2)}{s - m_Z^2 + im_Z \Gamma_Z} \left[ -\frac{1}{2} + \frac{1}{3} s_W^2 + \frac{s}{\Lambda^2} (c_W^2 c_{1L} + s_W^2 c_{3L}) \right] \quad (3)$$

$$G_{LR} = \frac{e^2}{s} \left[ \frac{1}{3} + \frac{s}{\Lambda^2} \tilde{c}_{3R} \right] + \frac{g_Z^2 (-\frac{1}{2} + s_W^2)}{s - m_Z^2 + im_Z \Gamma_Z} \left[ \frac{1}{3} s_W^2 + \frac{s}{\Lambda^2} s_W^2 \tilde{c}_{3R} \right] \quad (4)$$

$$G_{RL} = \frac{e^2}{s} \left[ \frac{1}{3} + \frac{s}{\Lambda^2} (-c_{1L} + c_{3L}) \right] + \frac{g_Z^2 (s_W^2)}{s - m_Z^2 + im_Z \Gamma_Z} \left[ -\frac{1}{2} + \frac{1}{3} s_W^2 + \frac{s}{\Lambda^2} (c_W^2 c_{1L} + s_W^2 c_{3L}) \right] \quad (5)$$

$$G_{RR} = \frac{e^2}{s} \left[ \frac{1}{3} + \frac{s}{\Lambda^2} \tilde{c}_{3R} \right] + \frac{g_Z^2 (s_W^2)}{s - m_Z^2 + im_Z \Gamma_Z} \left[ \frac{1}{3} s_W^2 + \frac{s}{\Lambda^2} s_W^2 \tilde{c}_{3R} \right] \quad (6)$$

$$G_{LS} = \frac{\sqrt{s} v_o}{\sqrt{2} \Lambda^2} \frac{g_Z^2 (-\frac{1}{2} + s_W^2)}{s - m_Z^2 + im_Z \Gamma_Z} [c_{Db}] \quad (7)$$

$$G_{RS} = \frac{\sqrt{s}v_o}{\sqrt{2}\Lambda^2} \frac{g_Z^2(s_W^2)}{s-m_Z^2+im_Z\Gamma_Z} [c_{Db}] \quad (8)$$

$$G_{LT} = \frac{\sqrt{2s}v_o}{\Lambda^2} \left\{ \frac{e^2}{s} [-c_{bW} + c_{bB}] + \frac{g_Z^2(-\frac{1}{2}+s_W^2)}{s-m_Z^2+im_Z\Gamma_Z} [c_W^2 c_{bW} + s_W^2 c_{bB}] \right\} \quad (9)$$

$$G_{RT} = \frac{\sqrt{2s}v_o}{\Lambda^2} \left\{ \frac{e^2}{s} [-c_{bW} + c_{bB}] + \frac{g_Z^2(s_W^2)}{s-m_Z^2+im_Z\Gamma_Z} [c_W^2 c_{bW} + s_W^2 c_{bB}] \right\}, \quad (10)$$

where  $s_W = \sin \theta_W$ ,  $c_W = \cos \theta_W$ , and  $g_Z = e/(s_W c_W)$ . Then for the process  $e^+e^- \rightarrow b\bar{b}$  we find

$$\sigma_F^b + \sigma_B^b = \frac{s}{16\pi} \{ |G_{LL}|^2 + |G_{LR}|^2 + |G_{RL}|^2 + |G_{RR}|^2 + |G_{LS} + G_{LT}|^2 + |G_{RS} + G_{RT}|^2 \\ - \frac{2m_b}{\sqrt{s}} \mathcal{R}e [(G_{LL} + G_{LR})(G_{LS} + 3G_{LT})^* + (G_{RL} + G_{RR})(G_{RS} + 3G_{RT})^*] \}, \quad (11)$$

$$\sigma_F^b - \sigma_B^b = \frac{3s}{64\pi} \{ |G_{LL}|^2 - |G_{LR}|^2 - |G_{RL}|^2 + |G_{RR}|^2 \\ - \frac{4m_b}{\sqrt{s}} \mathcal{R}e [(G_{LL} - G_{LR})G_{LT}^* - (G_{RL} - G_{RR})G_{RT}^*] \}, \quad (12)$$

where  $\sigma_F^b$  and  $\sigma_B^b$  are the forward and backward cross sections, and we have kept terms only up to first order in  $m_b/\sqrt{s}$ . We note that in Eqs. 11 and 12 there are  $1/\Lambda^4$  terms, and that for completeness one should in principle also include dimension-eight operators which can contribute to the process and are the same order in  $\Lambda$ . We do not include them here as we only wish to illustrate the importance and feasibility of studying such anomalous couplings.

On the  $Z$  resonance only the  $Z$  couplings contribute appreciably and we can define

$$G_{ij} \approx \frac{g_Z^2}{im_Z\Gamma_Z} g_i^e g_j^b, \quad i, j = L, R, S, T, \quad (13)$$

where

$$g_L^e = -\frac{1}{2} + s_W^2, \quad g_R^e = s_W^2, \quad (14)$$

$$g_L^b = -\frac{1}{2} + \frac{1}{3}s_W^2 + \frac{m_Z^2}{\Lambda^2}(c_W^2 c_{1L} + s_W^2 c_{3L}), \quad g_R^b = \frac{1}{3}s_W^2 + \frac{m_Z^2}{\Lambda^2}s_W^2 \tilde{c}_{3R}, \quad (15)$$

$$g_S^b = \frac{m_Z v_o}{\sqrt{2}\Lambda^2} c_{Db}, \quad g_T^b = \frac{\sqrt{2}m_Z v_o}{\Lambda^2} (c_W^2 c_{bW} + s_W^2 c_{bB}). \quad (16)$$

The measurables involving the  $b$  couplings on the  $Z$  resonance are the partial decay width

$$\frac{\Gamma_b}{\Gamma_b^{SM}} = \frac{[(g_L^b)^2 + (g_R^b)^2 + (g_T^b + g_S^b)^2 - \frac{2m_b}{m_Z}(g_L^b + g_R^b)(3g_T^b + g_S^b)]}{[(g_L^b)^2 + (g_R^b)^2]_{SM}}, \quad (17)$$

and the  $b$ -quark asymmetry

$$A_b = \frac{\left[ (g_L^b)^2 - (g_R^b)^2 - \frac{4m_b}{m_Z} (g_L^b - g_R^b) g_T^b \right]}{\left[ (g_L^b)^2 + (g_R^b)^2 + (g_T^b + g_S^b)^2 - \frac{2m_b}{m_Z} (g_L^b + g_R^b) (3g_T^b + g_S^b) \right]}, \quad (18)$$

where again we have kept terms up to first order in  $m_b/\sqrt{s}$ . The quantity  $\Gamma_b/\Gamma_b^{SM}$  can be determined from  $R_b = \Gamma_b/\Gamma_{had} = (\Gamma_b/\Gamma_b^{SM})/[(\Gamma_b/\Gamma_b^{SM}) + (1/R_b^{SM}) - 1]$ , assuming that the only deviation of the  $Z$  width from the SM occurs in  $\Gamma_b$ , and  $A_b$  can be determined from  $A_{FB}^b = \frac{3}{4}A_e A_b$  and  $A_e = [(g_L^e)^2 - (g_R^e)^2]/[(g_L^e)^2 + (g_R^e)^2]$ . The latest experimental measurements [6] are

$$R_b = 0.2178 \pm 0.0011, \quad A_b = 0.883 \pm 0.025, \quad (19)$$

where the Standard Model values are

$$R_b^{SM} = 0.2156, \quad A_b^{SM} = 0.936, \quad (20)$$

when  $\sin^2 \theta_W = 0.232$ . Both the  $R_b$  and  $A_b$  measurements are about 2-sigma from the standard model. The value for  $A_b$  in Eq. 19 is determined by combining the LEP and SLC results in quadrature; the LEP value is determined from the LEP measurements of  $A_{FB}^b$  and  $A_e$ , while the SLC value is measured directly using a forward-backward polarization asymmetry. A different LEP value of  $A_b$  can be found by using the LEP value for  $A_{FB}^b$  and the world average  $A_e$ , which then gives [6]

$$A_b = 0.867 \pm 0.022, \quad (21)$$

for the combined measurement. This alternative value of  $A_b$  is about 3-sigma away from the standard model value given in Eq. 20. We will not use the value in Eq. 21 in our analysis below, but will discuss briefly its consequences in Sec. V.

In Figs. 1 and 2 we show the regions allowed by the LEP1 and SLC data in Eq. 19 at 95% CL for various subsets of the parameters in the effective Lagrangian in Eq. 1. Six of the ten parameters affect  $e^+e^- \rightarrow b\bar{b}$ . Fig. 1 shows the allowed region for the parameters  $c_{3L}$  and the linear combination  $\tilde{c}_{3R} + c_{1L}c_W^2/s_W^2$ , and Fig. 2 for  $c_{Db}$  and the linear combination  $c_{bB} + c_{bW}c_W^2/s_W^2$ . The four parameters  $c_{3L}$ ,  $\tilde{c}_{3R}$ ,  $c_{Db}$ , and  $c_{bB}$  are suppressed by a factor

$s_W^2$  on the  $Z$  resonance, but not in their couplings to the photon. Hence they can give large effects at higher energies, such as at LEP2, where the photon contribution becomes important. Furthermore, the leading contributions of all six parameters which contribute to  $e^+e^- \rightarrow b\bar{b}$  will be enhanced by a factor of  $s/m_Z^2$  at higher energies compared to the  $Z$  resonance.

### III. LIMITS FROM PARTIAL WAVE UNITARITY

The unitarity limits on anomalous third-family couplings not constrained by  $e^+e^- \rightarrow b\bar{b}$  have been calculated in Ref. [9]. Here we determine the unitarity limits on all six anomalous couplings in Eq. 1; the details of the calculation are given in the Appendix. Despite the strong constraints from the data on the  $Z$  resonance, the energy dependence of these couplings implies that there will be significant constraints from unitarity as well. For  $c_{1L}$ ,  $c_{3L}$  and  $\tilde{c}_{3R}$ , the best limit from unitarity comes from the  $J = 1$  partial wave amplitude for the 2-to-2 processes involving the helicity channels  $b_+\bar{b}_-$ ,  $b_-\bar{b}_+$ ,  $t_+\bar{t}_-$ , and  $t_-\bar{t}_+$ . The largest eigenvalue of the  $4 \times 4$  coupled-channel matrix leads to the strongest constraint. Although the exact expressions are somewhat messy, if we keep only the terms quadratic in the anomalous couplings that are enhanced by a factor  $s^2/\Lambda^4$  at high energies, the unitarity condition can be written approximately as

$$\tilde{c}_{3R}^2 + 2c_{3L}^2 < \frac{2c_W^2}{\alpha} \frac{\Lambda^4}{s^2} \approx \left( \frac{14 \text{ TeV}^2}{s} \right)^2, \quad (22)$$

$$|c_{1L}| < \frac{s_W}{\sqrt{\alpha}} \frac{\Lambda^2}{s} \approx \frac{5.5 \text{ TeV}^2}{s}, \quad (23)$$

where we have used  $\Lambda = 1 \text{ TeV}$ . For  $c_{Db}$ ,  $c_{bB}$  and  $c_{bW}$ , the best limit from unitarity comes from the  $J = 0$  partial wave amplitude for the processes involving the channels  $b_+\bar{b}_+$  and  $b_-\bar{b}_-$ . The largest eigenvalue of the  $2 \times 2$  coupled-channel matrix leads to the strongest constraint. Keeping only the leading terms for each coupling, we find the constraint

$$34c_{Db}^2 + 9\frac{m_Z^2}{s}[8(c_{bB}s_W^2 + c_{bW}c_W^2) - c_{Db}]^2 < \frac{768s_W^2c_W^2}{\alpha} \frac{m_Z^2}{v_o^2} \frac{\Lambda^4}{s^2} \approx \left( \frac{49 \text{ TeV}^2}{s} \right)^2. \quad (24)$$

The unitarity constraints for  $\Lambda = 1$  TeV are shown in Figs. 3 and 4 for  $\sqrt{s} = 1, 2$ , and 3 TeV. The limits from LEP1 and the SLC are also shown for comparison.

#### IV. EFFECTS ON $B\bar{B}$ PRODUCTION AT LEP2

The next step is to determine the range of measurements at LEP2 that are possible which are also consistent with the LEP and SLC data. From Eqs. 3 to 12 we note that to leading order in  $s$ , the anomalous interactions have contributions proportional to  $s/\Lambda^2$  (from the interference of SM and anomalous pieces in  $G_{LL}$ ,  $G_{LR}$ ,  $G_{RL}$ , and  $G_{RR}$ ) and  $sv_o^2/\Lambda^4$  (from  $G_{LS}$ ,  $G_{LS}$ ,  $G_{LT}$ , and  $G_{RT}$ ). These contributions can therefore lead to large deviations from the SM at higher energies. In our analysis, we study the operators which involve vector and axial vector couplings ( $c_{1L}$ ,  $c_{3L}$ , and  $\tilde{c}_{3R}$ ) separately from those which introduce scalar and tensor couplings ( $c_b B$ ,  $c_{bW}$ , and  $c_{Db}$ ). In Fig. 5 we show the range of measurements possible for  $\sigma_b \equiv \sigma(e^+e^- \rightarrow b\bar{b})$  and  $A_{FB,b} \equiv (\sigma_{F,b} - \sigma_{B,b})/(\sigma_{F,b} + \sigma_{B,b})$  at LEP2, given the constraints on the parameters from LEP and SLC data and partial wave unitarity with the new physics scale set at 1 TeV.

Fig. 5a shows the possible range of measurements at LEP2 with  $\sqrt{s} = 170$  GeV for  $\Delta A_{FB}/A_{FB} \equiv (A_{FB,b} - A_{FB,b}^{SM})/A_{FB,b}^{SM}$  and  $\Delta\sigma/\sigma \equiv (\sigma_b - \sigma_b^{SM})/\sigma_b^{SM}$  when  $c_{3L}$  and  $\tilde{c}_{3R}$  are varied over their allowed values, for  $c_{1L} = 1, 0$ , and  $-1$  (larger values of  $c_{1L}$  are not allowed by unitarity). The horizontal grid lines correspond to constant values of  $c_{3L}$ , while the vertical grid lines correspond to constant values of  $\tilde{c}_{3R}$ . We see that sizeable deviations from the standard model are possible, up to 60% in  $\sigma$  and 40% in  $A_{FB}$ . Even larger deviations are possible if  $A_b$  from Eq. 21 is used. The corresponding ranges for  $\sqrt{s} = 190$  and 200 GeV are shown in Figs. 5b and 5c, respectively. A comparison of the graphs in Fig. 5 shows that the deviations grow with  $\sqrt{s}$ , as expected from the  $s$  dependence of the anomalous contributions.

In principle one should be able to deduce the three values of the anomalous parameters  $c_{1L}$ ,  $c_{3L}$ , and  $\tilde{c}_{3R}$  from the combined measurements of  $\sigma_b$  and  $A_{FB}^b$  taken at different ener-



gies. As an illustration, let's assume that the measurements  $\Delta\sigma/\sigma = 0.07, 0.09, 0.11$ , and  $\Delta A_{FB}/A_{FB} = -0.08, -0.10, -0.11$  are taken at  $\sqrt{s} = 170, 190$ , and  $200$  GeV, respectively. Assuming an integrated luminosity of  $10 \text{ fb}^{-1}$  at each energy, the standard statistical errors are  $\delta\sigma_b/\sigma_b = 1/\sqrt{N} \approx .04$ , and  $\delta A_{FB,b} = 2\sqrt{N_F N_B/N^3} \approx .04$ , where  $N_F$  and  $N_B$  are the number of forward and backward  $b\bar{b}$  events, respectively, and  $N = N_F + N_B$ . Then the best least-squares fit to the anomalous parameters is  $c_{1L} = 0.0 \pm 0.2$ ,  $c_{3L} = -1.70^{+0.28}_{-0.13}$ , and  $\tilde{c}_{3R} = 2.70^{+0.16}_{-0.65}$ . From this exercise it is clear that the combined measurements of  $\sigma_b$  and  $A_{FB}^b$  taken at different energies at LEP2 is sufficient to greatly constrain the parameter space, and, if the deviations from the standard model are large enough, provide strong evidence for new physics involving the third generation fermions.

We have done a similar analysis for the parameters involving the scalar and tensor interactions,  $c_{bB}$ ,  $c_{bW}$ , and  $c_{Db}$ . In Fig. 6a we show the possible range of measurements at LEP2 with  $\sqrt{s} = 170$  GeV for  $\Delta A_{FB}/A_{FB}$  and  $\Delta\sigma/\sigma$  when  $c_{bB}$  and  $c_{Db}$  are varied over their allowed values, for  $c_{bW} = 2, 0$ , and  $-2$  (larger values of  $c_{bW}$  are not allowed by unitarity). Fig. 6b shows the corresponding ranges for  $c_{bW} = 1$  and  $-1$ . We see from Fig. 6 that the range of deviations from the standard model is not as large as in Fig. 5, and there is more ambiguity as to which combinations of parameters yield a certain set of measurements. Also, for the parameters which introduce scalar and tensor couplings there is a weaker  $\sqrt{s}$  dependence, which makes a precise determination of their exact values more difficult than the case involving vector and axial vector couplings.

## V. DISCUSSION

We have found the constraints on a class of six dimension-6 operators involving  $b$ -quarks with derivative couplings from LEP and SLC data and from partial wave unitarity. We have also shown that these operators may lead to large deviations from the standard model predictions for the total cross section and forward-backward asymmetry in  $b\bar{b}$  production at LEP2. The effect of the dimension-six operators with derivative coupling at LEP2 has been

discussed in Ref. [10], and the three vector and axial vector operators have also been studied in detail in Ref. [11] for LEP2 and NLC energies. In our analysis we show that precise measurements of the  $b\bar{b}$  cross section together with the forward-backward asymmetry *at different energies* can greatly limit the possible range of anomalous couplings which might be responsible for the deviations. If these anomalous operators are in fact present, even larger deviations can be expected at the much higher energy scale of the NLC [11].

## VI. ACKNOWLEDGEMENTS

We thank A. Firestone and E. Rosenberg for discussions. This work was supported in part by the U.S. Department of Energy under Contracts DE-FG02-94ER40817 and DE-FG02-92ER40730. XZ was supported in part by the National Science foundation of China.

## VII. APPENDIX: BOUNDS FROM PARTIAL WAVE UNITARITY

In this Appendix we describe in more detail the derivation of the bounds on the anomalous couplings from partial wave unitarity. In each case we consider contributions which are quadratic in the anomalous couplings, and treat the couplings for the vector and axial vector interactions separately from those for the scalar and tensor interactions.

For the parameters  $c_{1L}$ ,  $c_{3L}$ , and  $\tilde{c}_{3R}$ , the best limit from partial wave unitarity comes from the color singlet  $J = 1$  amplitudes. The  $J = 1$  helicity amplitudes for the processes which are quadratic in the anomalous couplings are, to leading order in  $s$ ,

$$T_1(b_+\bar{b}_- \rightarrow b_+\bar{b}_-) = \frac{11}{24} \frac{\alpha}{c_W^2} \frac{s^2}{\Lambda^4} \tilde{c}_{3R}^2, \quad (25)$$

$$T_1(t_+\bar{t}_- \rightarrow t_+\bar{t}_-) = T_1(b_+\bar{b}_- \leftrightarrow t_+\bar{t}_-) = 0 \quad (26)$$

$$T_1(b_-\bar{b}_+ \rightarrow b_-\bar{b}_+) = T_1(t_-\bar{t}_+ \rightarrow t_-\bar{t}_+) = \frac{11}{24} \frac{\alpha}{c_W^2} \frac{s^2}{\Lambda^4} \left( c_{3L}^2 + c_{1L}^2 \frac{c_W^2}{s_W^2} \right), \quad (27)$$

$$T_1(b_-\bar{b}_+ \leftrightarrow t_-\bar{t}_+) = \frac{\alpha}{c_W^2} \frac{s^2}{\Lambda^4} \left( \frac{1}{2} c_{3L}^2 - \frac{7}{12} c_{1L}^2 \frac{c_W^2}{s_W^2} \right), \quad (28)$$

$$T_1(b_+\bar{b}_- \leftrightarrow b_-\bar{b}_+) = T_1(b_+\bar{b}_- \leftrightarrow t_-\bar{t}_+) = -\frac{1}{2} \frac{\alpha}{c_W^2} \frac{s^2}{\Lambda^4} c_{3L} \tilde{c}_{3R}, \quad (29)$$

$$T_1(t_+\bar{t}_- \leftrightarrow b_-\bar{b}_+) = \frac{1}{8} \frac{\alpha}{c_W^2} \frac{s^2}{\Lambda^4} \frac{m_t^2}{m_Z^2} c_{1L}^2 \frac{c_W^2}{s_W^2}, \quad (30)$$

$$T_1(t_+\bar{t}_- \leftrightarrow t_-\bar{t}_+) = \frac{1}{16} \frac{\alpha}{c_W^2} \frac{s^2}{\Lambda^4} \frac{m_t^2}{m_Z^2} \left( c_{3L}^2 + c_{1L}^2 \frac{c_W^2}{s_W^2} \right), \quad (31)$$

$$(32)$$

where terms involving  $m_b/m_Z$  or smaller have been dropped. The best constraint comes from the eigenvalues of the coupled channel matrix. An approximate solution can be found by ignoring the  $m_t^2/m_W^2$  terms (which are suppressed somewhat by small coefficients), and replacing the terms with coefficients 11/24 and 7/12 by terms with coefficients of 1/2. Then the coupled channel matrix for the  $J = 1$  partial wave amplitude in the  $b_+\bar{b}_-$ ,  $t_+\bar{t}_-$ ,  $b_-\bar{b}_+$ ,  $t_-\bar{t}_+$  basis is

$$a_1 = \frac{1}{2} \frac{\alpha}{c_W^2} \frac{s^2}{\Lambda^4} \begin{pmatrix} \tilde{c}_{3R}^2 & 0 & -c_{3L}\tilde{c}_{3R} & -c_{3L}\tilde{c}_{3R} \\ 0 & 0 & 0 & 0 \\ -c_{3L}\tilde{c}_{3R} & 0 & c_{3L}^2 + c_{1L}^2 \frac{c_W^2}{s_W^2} & c_{3L}^2 - c_{1L}^2 \frac{c_W^2}{s_W^2} \\ -c_{3L}\tilde{c}_{3R} & 0 & c_{3L}^2 - c_{1L}^2 \frac{c_W^2}{s_W^2} & c_{3L}^2 + c_{1L}^2 \frac{c_W^2}{s_W^2} \end{pmatrix}. \quad (33)$$

The eigenvalues of the matrix in Eq. 33 are

$$\lambda = 0, \quad 0, \quad \frac{\alpha}{c_W^2} \frac{s^2}{\Lambda^4} c_{1L}^2 \frac{c_W^2}{s_W^2}, \quad \frac{1}{2} \frac{\alpha}{c_W^2} \frac{s^2}{\Lambda^4} (2c_{3L}^2 + \tilde{c}_{3R}^2). \quad (34)$$

The approximate partial wave unitarity bounds in Eqs. 22 and 23 are determined by requiring that the coupled channel eigenvalues be less than unity.

For the parameters  $c_{bB}$ ,  $c_{bW}$ , and  $c_{Db}$ , the best limit from partial wave unitarity comes from the color singlet  $J = 0$  amplitudes. The  $J = 0$  amplitudes for the processes which are quadratic in the anomalous couplings are, to leading order in  $s$ ,

$$T_o(b_+\bar{b}_+ \rightarrow b_+\bar{b}_+) = T_o(b_-\bar{b}_- \rightarrow b_-\bar{b}_-) = -\frac{3}{128} \frac{\alpha}{s_W^2 c_W^2} \frac{s^2}{\Lambda^4} \frac{v_0^2}{m_Z^2} c_{Db}^2, \quad (35)$$

$$T(b_+\bar{b}_+ \leftrightarrow b_-\bar{b}_-) = -\frac{1}{768} \frac{\alpha}{s_W^2 c_W^2} \frac{s^2}{\Lambda^4} \left[ 9 \frac{m_Z^2}{s} (8c_{bB}s_W^2 + 8c_{bW}c_W^2 - c_{Db})^2 + 16c_{Db}^2 \right]. \quad (36)$$

These may be summarized by the  $J = 0$  coupled channel matrix in the  $b_+\bar{b}_+$ ,  $b_-\bar{b}_-$  basis

$$a_0 = -\frac{1}{768} \frac{\alpha}{s_W^2 c_W^2} \frac{s^2}{\Lambda^4} \begin{pmatrix} 18c_{Db}^2 & 9 \frac{m_Z^2}{s} c^2 + 16c_{Db}^2 \\ 9 \frac{m_Z^2}{s} c^2 + 16c_{Db}^2 & 18c_{Db}^2 \end{pmatrix}, \quad (37)$$

where  $c \equiv 8c_{bB}s_W^2 + 8c_{bW}c_W^2 - c_{Db}$ . There are diagrams quadratic in the couplings which contribute to processes such as  $t\bar{t} \leftrightarrow b\bar{b}$ , but the leading term in  $s$  for these amplitudes are  $J = 1$ , and give a looser constraint. There are also diagrams which are quadratic in couplings that do not affect LEP1 and SLC measurables but contribute to processes such as  $t\bar{t} \leftrightarrow t\bar{t}$ . Since in this paper we are primarily interested in only operators constrained by LEP1 and the SLC, we do not include the effects of these other operators. As before, the partial wave unitarity bound in Eq. 24 is determined by requiring that the maximum coupled channel eigenvalue be less than unity (the smallest eigenvalue in this case always gives a looser constraint).

## REFERENCES

- [1] For a recent review, see, G. Altarelli, hep-ph/9611239.
- [2] R.D. Peccei and X. Zhang, Nucl. Phys. **B337**, 269 (1990); R.D. Peccei, S. Peris and X. Zhang, *ibid.* **B349**, 305 (1991); C. Hill and S. Parke, Phys. Rev. D **49**, 4454 (1994); D. Atwood, A. Kagan and T. Rizzo, Phys. Rev. **52**, 6264 (1995); D.O. Carlson, E. Malkawi and C.-P. Yuan, Phys. Lett. **B337**, 145 (1994); H. Georgi, et al, Phys. Rev. **D51**, 3888 (1995); T. Han, R.D. Peccei and X. Zhang, Nucl. Phys. **B454**, 527 (1995); B.-L. Young and X. Zhang, Phys. Rev. **D51**, 6564 (1995); S. Dawson and G. Valencia, Phys. Rev. **D53**, 1721 (1996); C.T. Hill and X. Zhang Phys. Rev. **D51**, 3563 (1995); R.S. Chivukula, S.B. Selipsky and H. Simmons, Phys. Rev. Lett. **69**, 575 (1992); P. Haberl, O. Nachtman and A. Wilch, Phys. Rev. **D53**, 4875 (1996); T. Han, K. Whisnant, B.-L. Young and X. Zhang, Phys. Lett. **B385**, 311 (1996); G. Gounaris, F. Renard and C. Verzegnassi, Phys. Rev. **D52**, 451 (1995); A. Datta and X. Zhang, Phys. Rev. **D55**, 2530 (1997).
- [3] F. Abe et al. (CDF Collaboration), Phys. Rev. Lett. **74**, 2626 (1995); S. Abachi et al. (D0 Collaboration, Phys. Rev. Lett. **74**, 2632 (1995).
- [4] For a recent review, see, e.g., H. Neuberger, in *Proceedings of the XXVI International Conference on High Energy Physics*, Dallas, Texas, 1992, edited by J. Sanford, AIP Conf. Proc. No. 272 (AIP, New York, 1992), Vol. II, p. 1360.
- [5] G. 't Hooft, in *Recent Developments in Gauge Theories*, Proceedings of the Cargese Summer Institute, Cargese, France, 1979, edited by G. 't Hooft et al., NATO Advanced Study Institute Series B; Physics Vol. 59 (Plenum, New York, 1980).
- [6] A. Blondel, in the *Proceedings of the XXVIIIth International Conference on High Energy Physics*, Warsaw, Poland, 1996, ed. by Z. Ajduk and A.K. Wroblewski (World Scientific, Singapore, 1997), p. 205.
- [7] For example, see, A. Datta, B.-L. Young and X. Zhang, Phys. Lett. **B385**, 225 (1996).
- [8] For example, see, R.S. Chivukula, B.A. Dobrescu and E.H. Simmons, hep-ph/9702416.
- [9] G.J. Gounaris, D.T. Papadamou, and F.M. Renard, preprint hep-ph/9609437, October 1996.

- [10] K. Whisnant, Jinmin Yang, Bing-Lin Young, and X. Zhang, preprint hep-ph/9702305, to appear in Phys. Rev. D.
- [11] During preparation of this manuscript we received a preprint by G.J. Gounaris, D.T. Papadamou, and F.M. Renard, preprint hep-ph/9703281, March 1997, which also examines the effect of the operators moderated by the couplings  $c_{1L}$ ,  $c_{3L}$  and  $\tilde{c}_{3R}$ .

## FIGURE CAPTIONS

FIG. 1. 95% CL constraints from  $R_b$  (dash-dotted lines) and  $A_b$  (dashed lines) for the parameters  $\tilde{c}_{3R}$  versus  $c_{3L} + c_{1L}c_W^2/s_W^2$ . The regions where the bands overlap are indicated by the solid lines. The data are taken from Ref. [6].

FIG. 2. 95% CL constraints from  $R_b$  (dash-dotted lines) and  $A_b$  (dashed lines) for the parameters  $c_{Db}$  versus  $c_{bB} + c_{bW}c_W^2/s_W^2$ . The notation and data used are the same as in Fig. 1.

FIG. 3. Constraints from partial wave unitarity for  $\sqrt{s}=1$  TeV (solid lines), 2 TeV (dash-dotted lines), and 3 TeV (dashed lines) for  $\tilde{c}_{3R}$  versus  $c_{3L}$ , with  $\Lambda = 1$  TeV. The regions inside the curves are allowed. The regions allowed by LEP and SLC data at 95% CL, taken from Fig. 1, are also shown. The allowed regions are shown for three different values of  $c_{1L}$ .

FIG. 4. Constraints from partial wave unitarity for  $\sqrt{s}=1$  TeV (solid lines), 2 TeV (dash-dotted lines), and 3 TeV (dashed lines) for  $c_{bB} + c_{bW}c_W^2/s_W^2$  versus  $c_{Db}$ , with  $\Lambda = 1$  TeV. The regions inside the curves are allowed. The regions allowed by LEP and SLC data at 95% CL, taken from Fig. 2, are also shown.

FIG. 5 Possible range of measurements for  $\Delta A_{FB}/A_{FB}$  and  $\Delta\sigma/\sigma$  at LEP2 with (a)  $\sqrt{s} = 170$  GeV, (b)  $\sqrt{s} = 190$  GeV, and (c)  $\sqrt{s} = 200$  GeV, given the constraints from LEP, the SLC, and partial wave unitarity when  $\sqrt{s} = \Lambda = 1$  TeV. The horizontal grid lines correspond to constant values of  $c_{3L}$ , while the vertical grid lines correspond to constant values of  $\tilde{c}_{3R}$ , while  $c_{1L}$  is held fixed at 1, 0, and  $-1$ . The points marked by a dot correspond to  $c_{3L} = -1.7$  and  $\tilde{c}_{3R} = 2.7$  in each case, and the space between grid lines corresponds to a change of 0.1 and 0.5 in  $c_{3L}$  and  $\tilde{c}_{3R}$ , respectively.

FIG. 6 Possible range of measurements for  $\Delta A_{FB}/A_{FB}$  and  $\Delta\sigma/\sigma$  at LEP2 with  $\sqrt{s} = 170$  GeV when  $c_{bB}$  and  $c_{Db}$  are varied, given the constraints from LEP, the SLC, and partial wave unitarity when  $\sqrt{s} = \Lambda = 1$  TeV. The ranges are shown for (a)  $c_{bW} = 2.0, 0.0$ , and  $-2.0$ , and (b)  $c_{bW} = 1.0$  and  $-1.0$ .

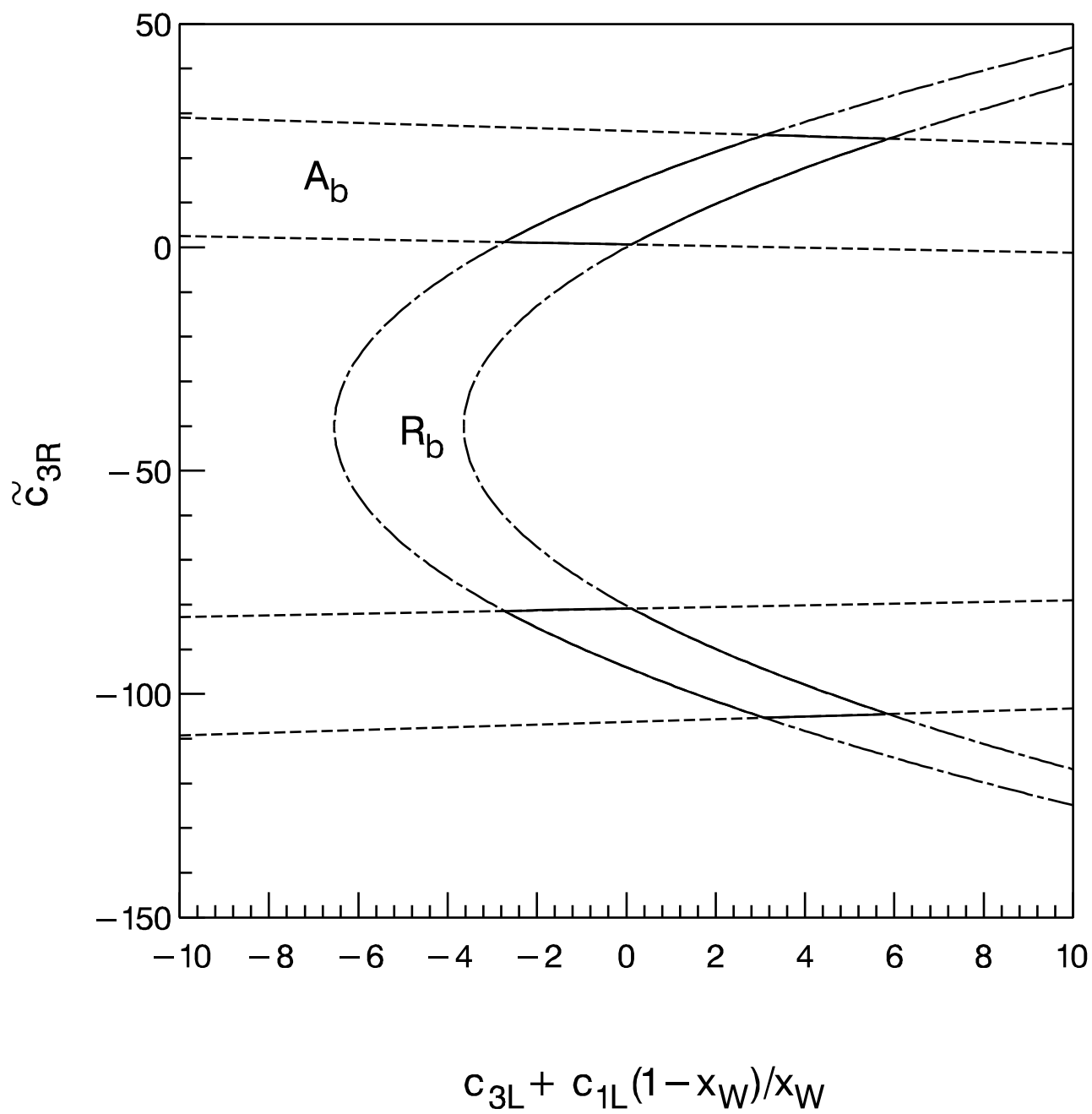


Fig. 1



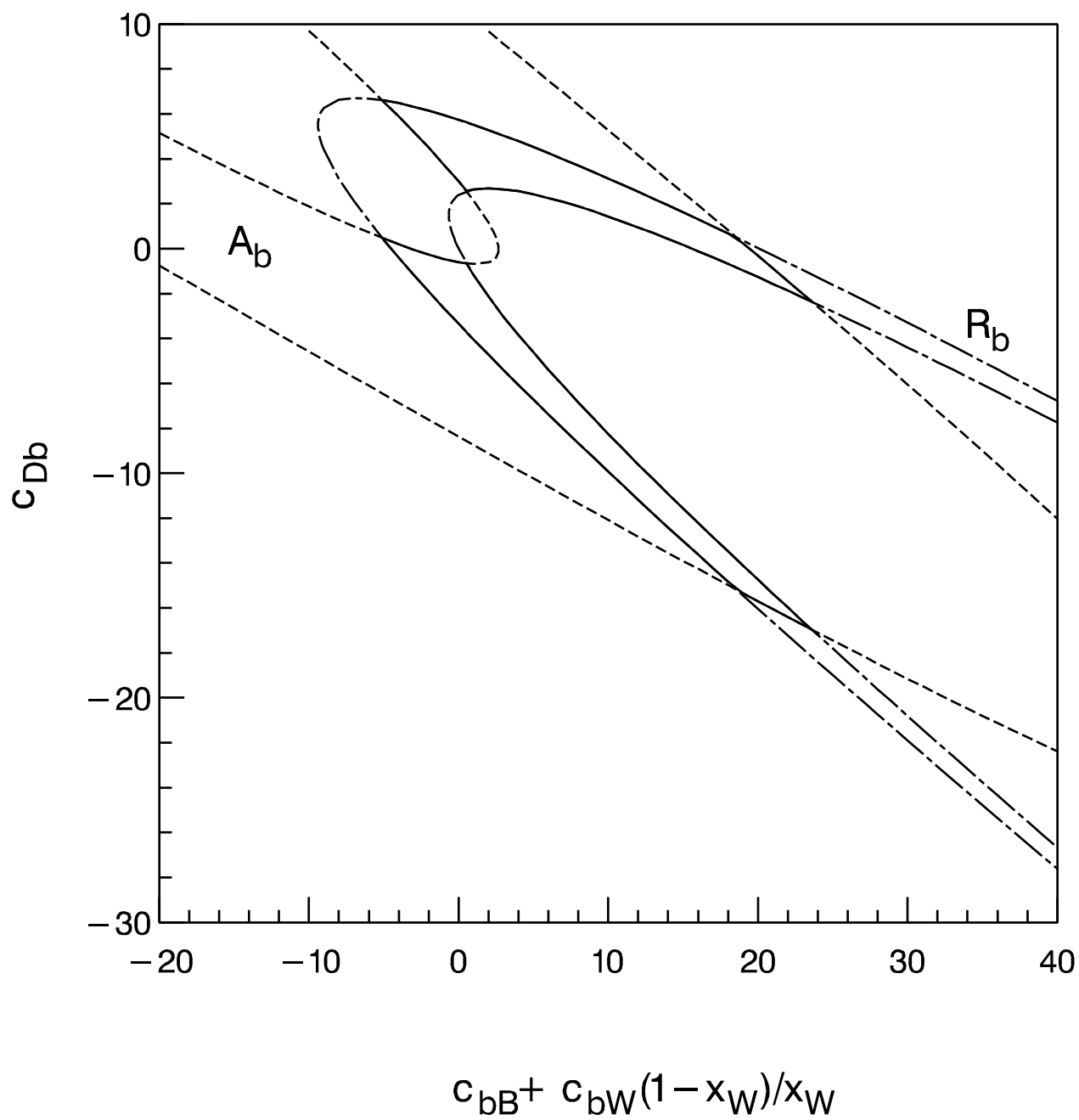


Fig. 2

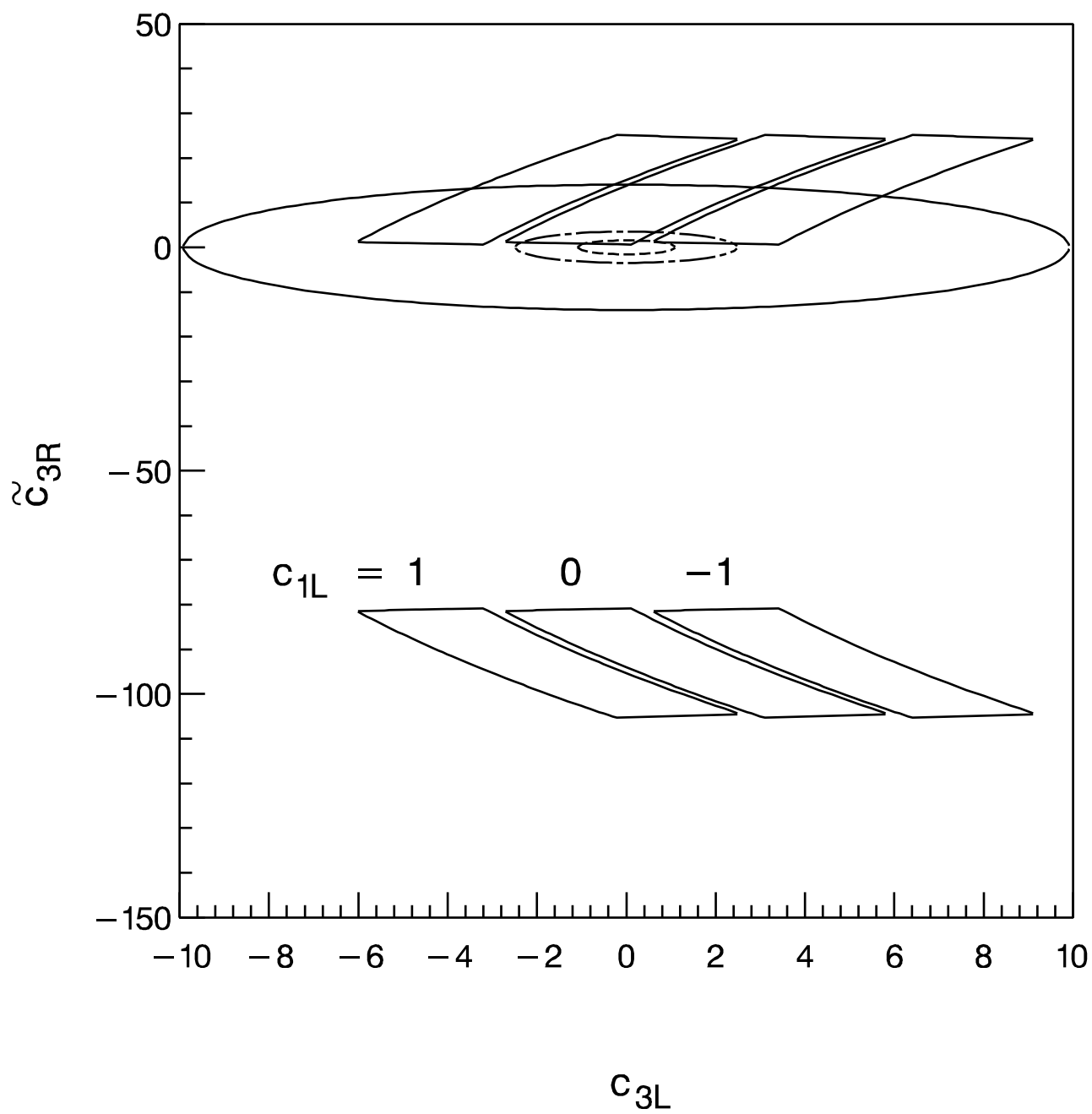


Fig. 3

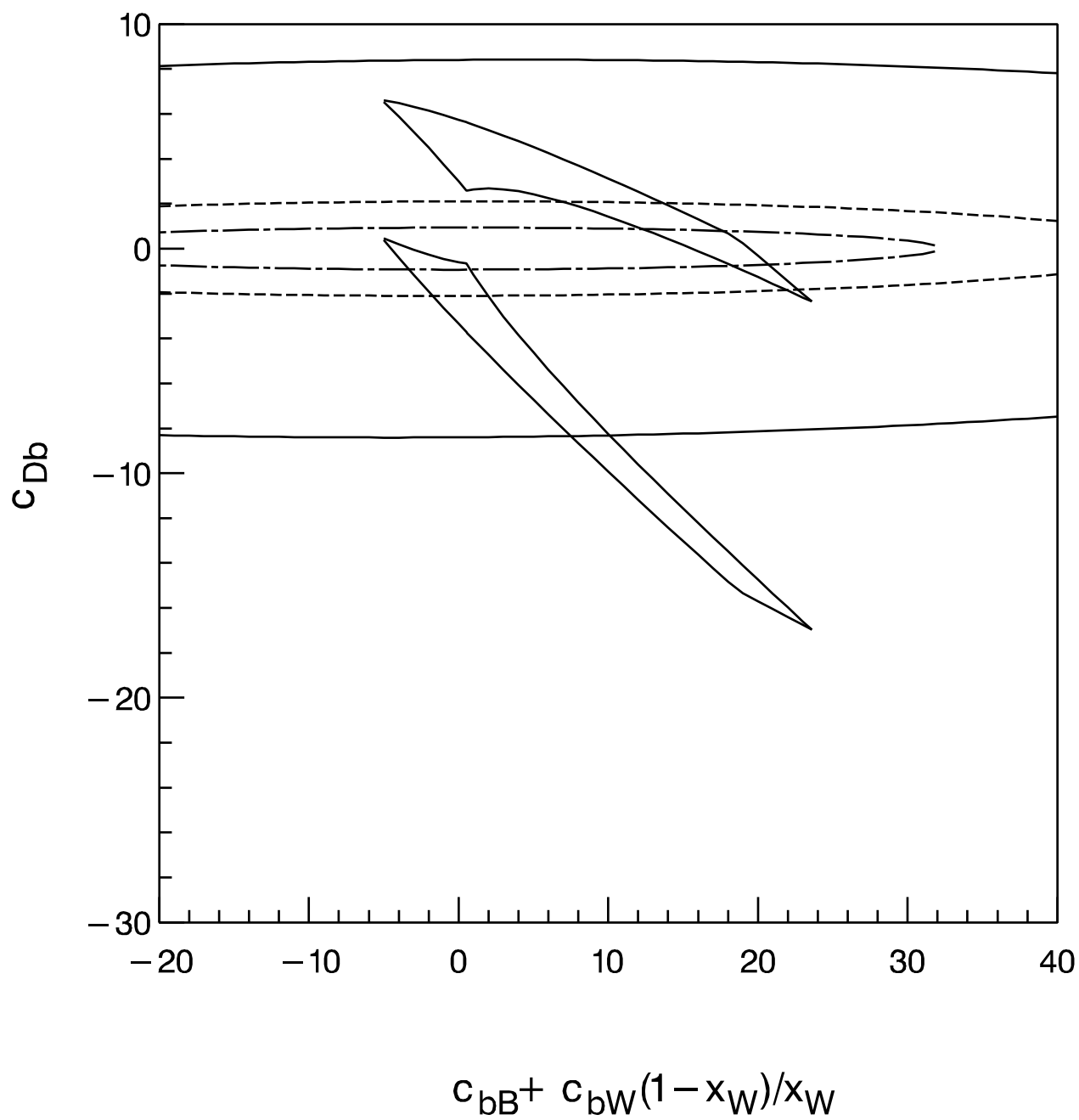


Fig. 4

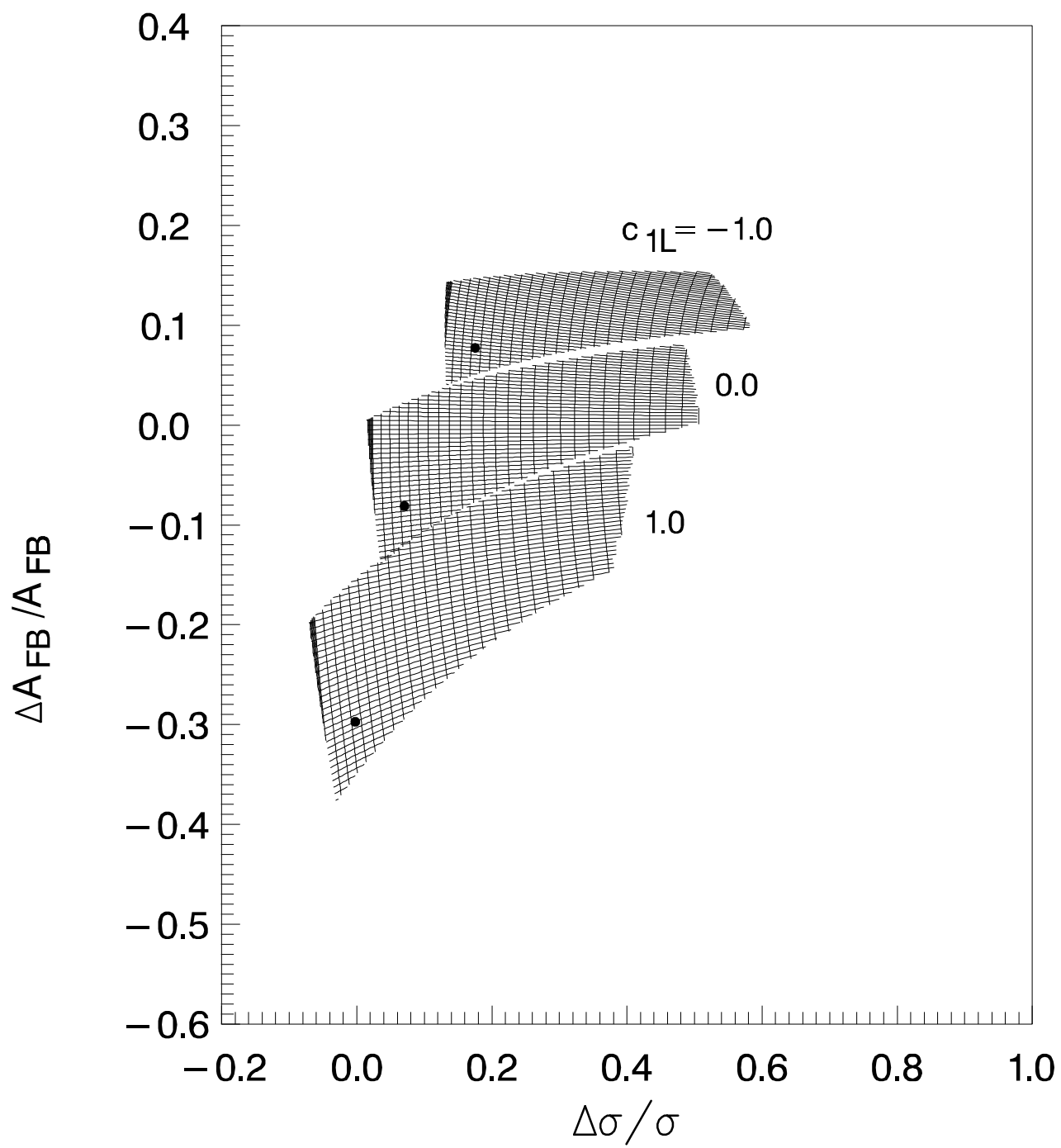


Fig. 5a

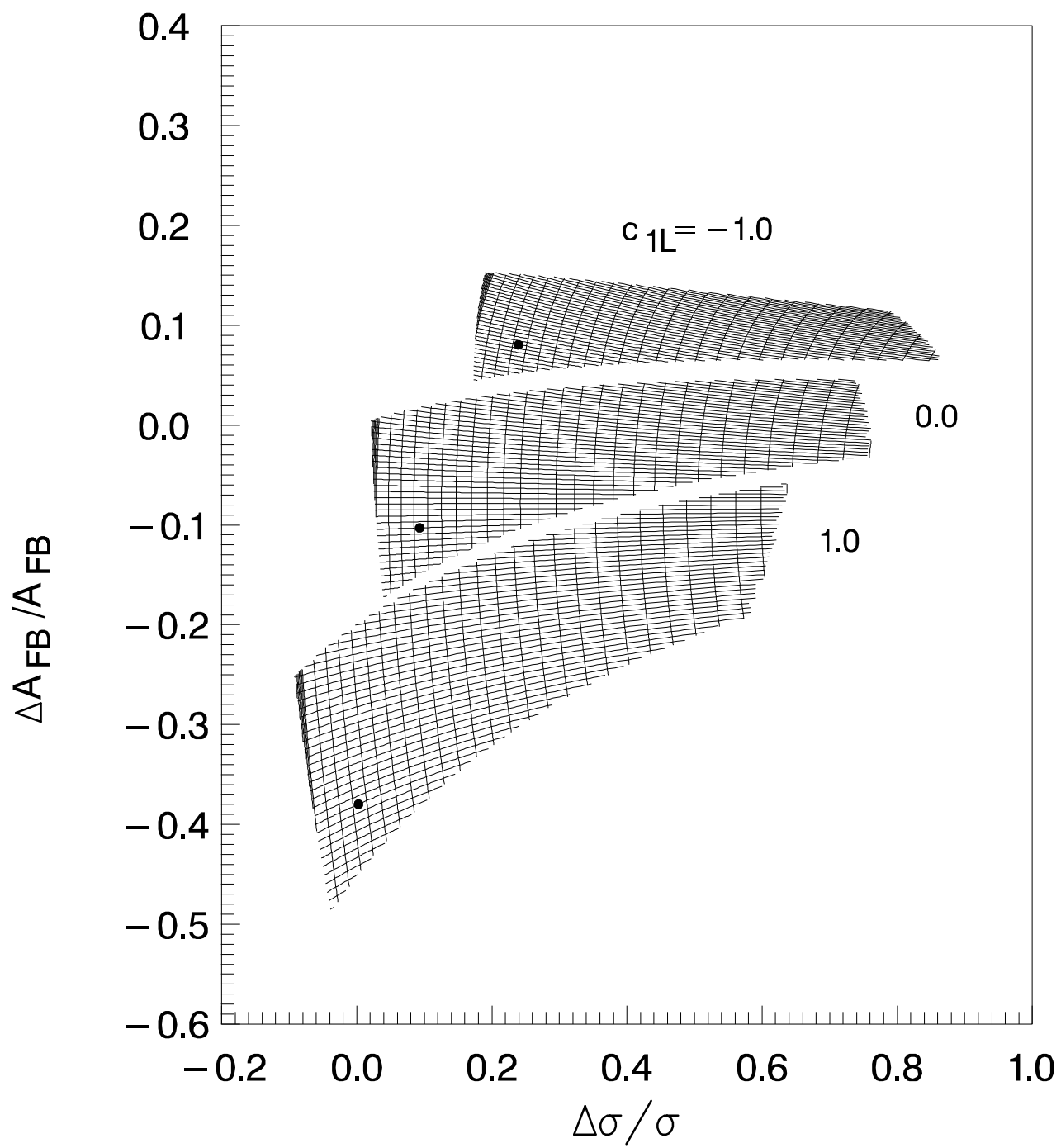


Fig. 5b

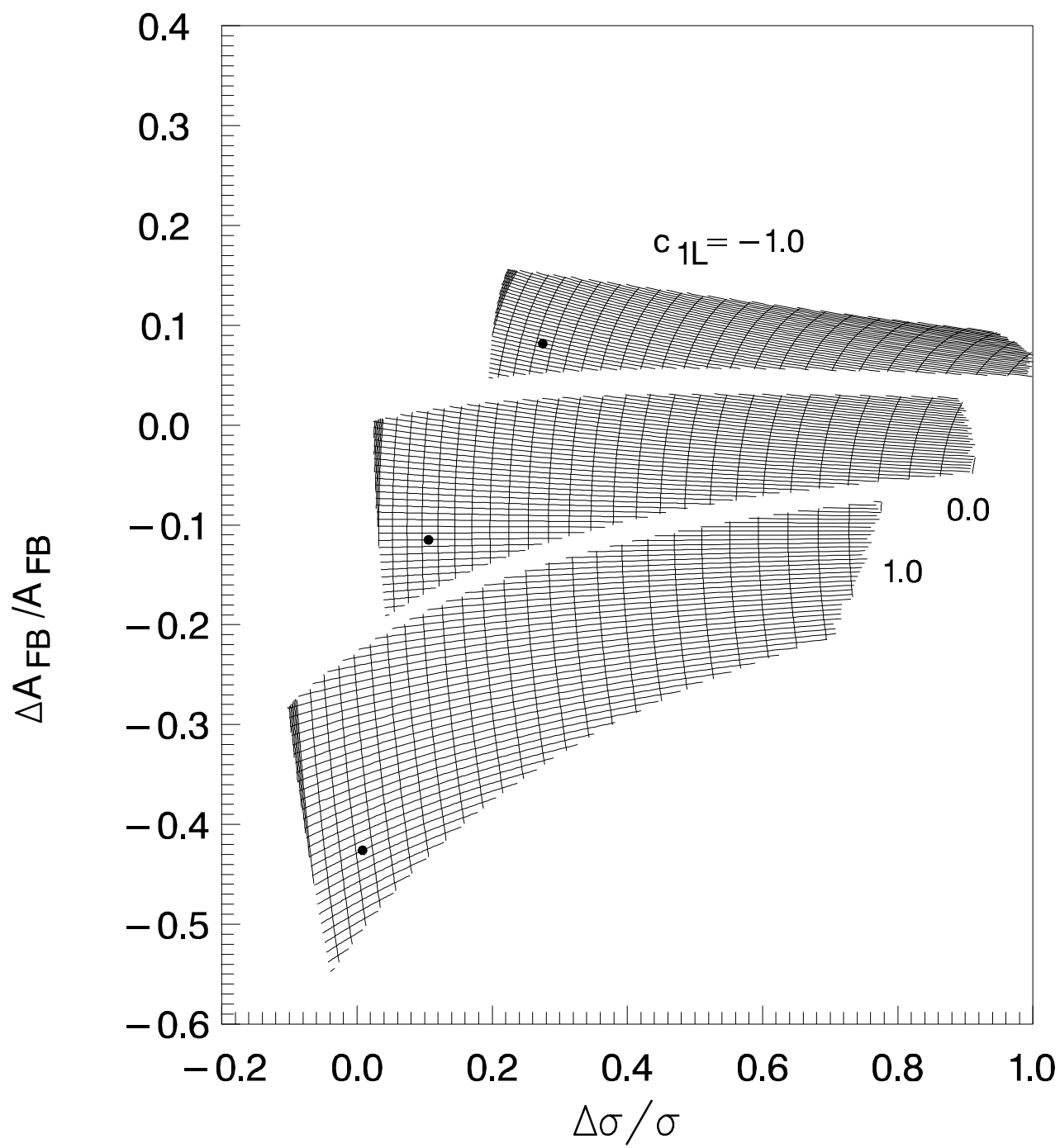


Fig. 5c

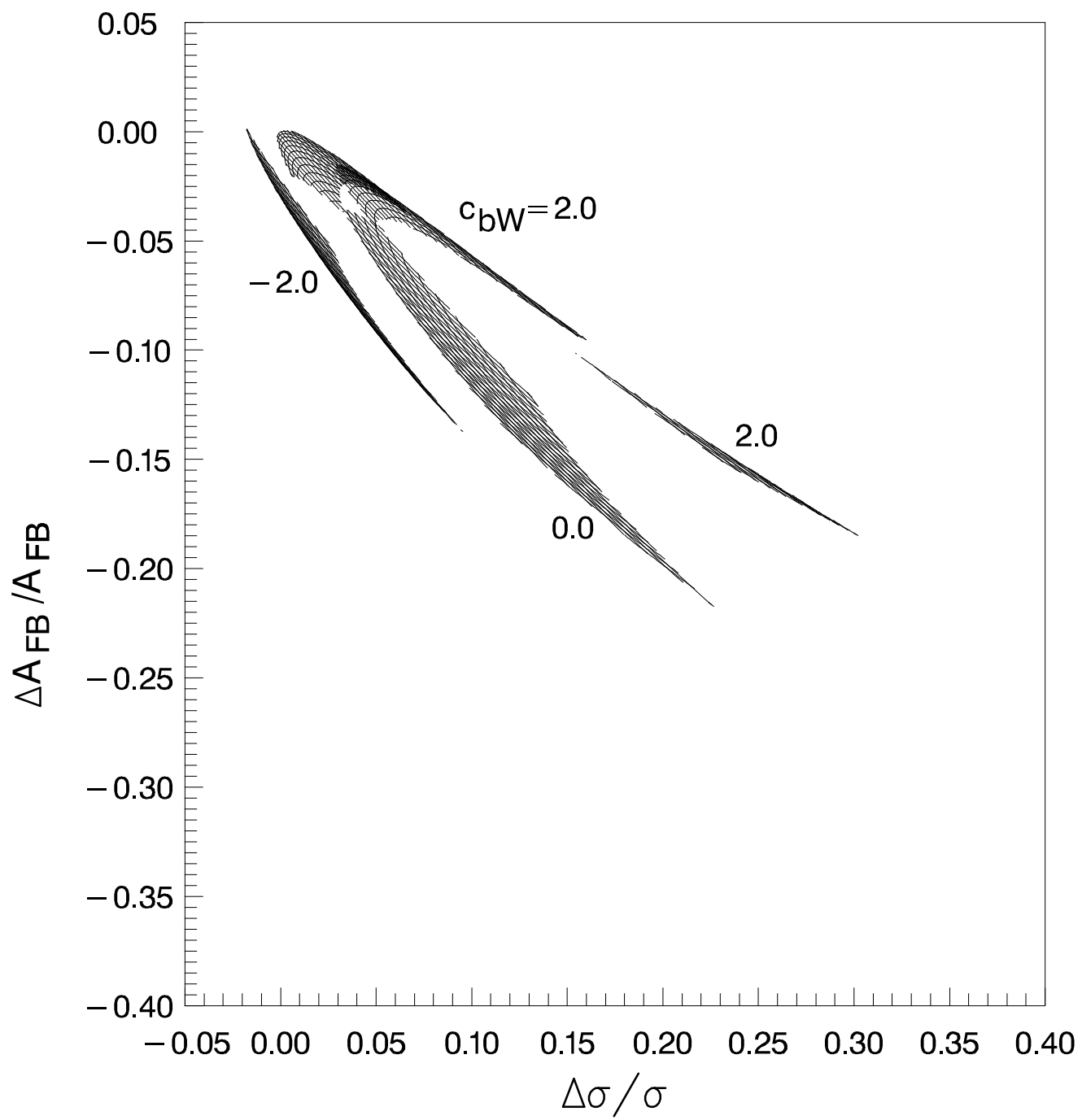


Fig. 6a

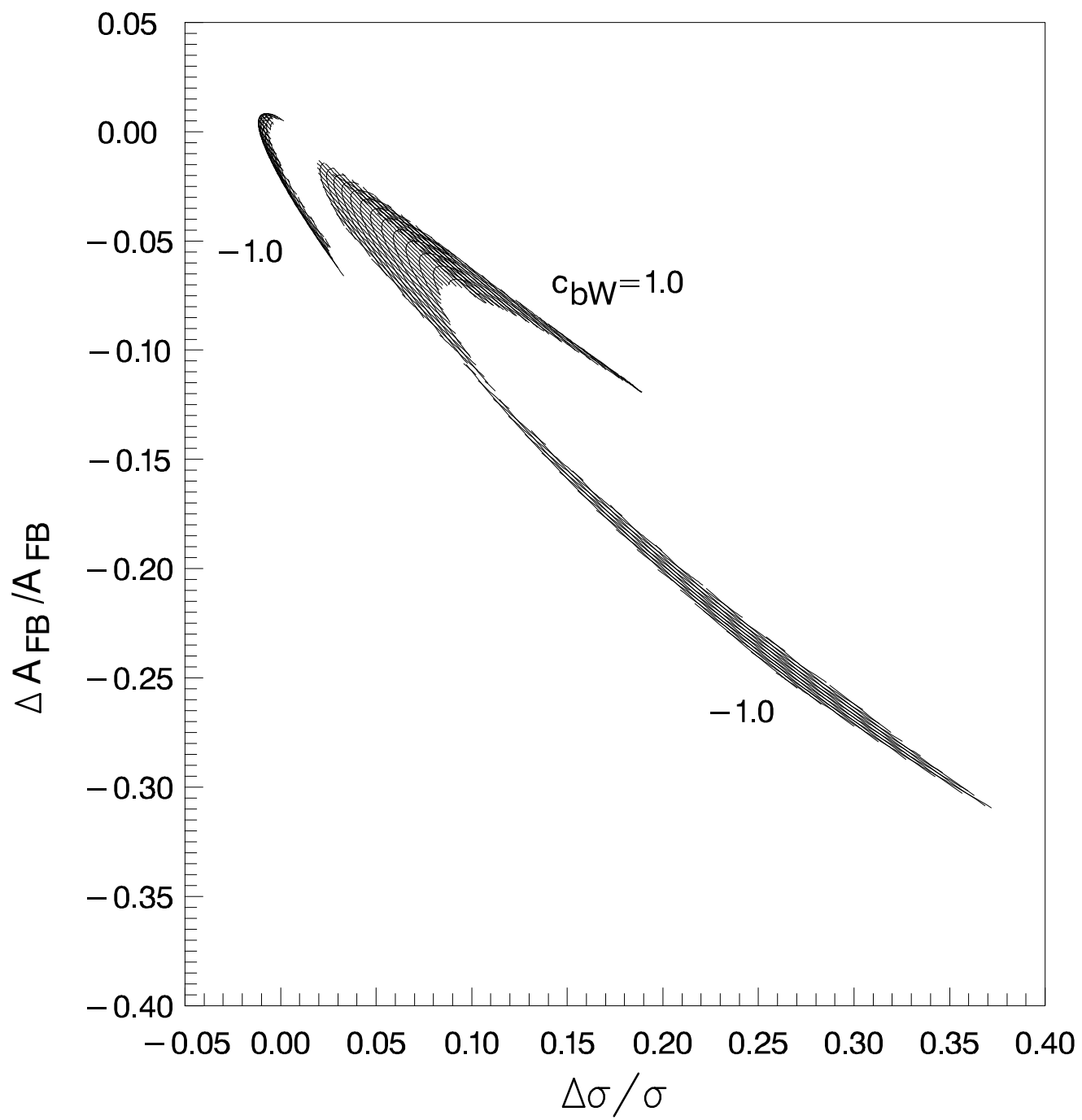


Fig. 6b